Peierls transition with acoustic phonons and twist deformation in carbon nanotubes

Figge, M. T.; Mostovoy, M. V.; Knöster, J.

Published in:
ArXiv

Publication date:
1999

Peierls transition with acoustic phonons and twist deformation in carbon nanotubes

Marc Thilo Figge, Maxim Mostovoy, and Jasper Knoester
Institute for Theoretical Physics and Materials Science Center
University of Groningen, Nijenborgh 4, 9747 AG Groningen, The Netherlands
(June 28, 2006)

We consider the Peierls instability due to the interaction of electrons with both acoustic and optical phonons. We suggest that such a transition takes place in carbon nanotubes with small radius. The topological excitations and the temperature dependence of the conductivity resulting from the electron-lattice interactions are considered.

PACS numbers: 63.20.Kr, 63.70.+h, 05.45.Yv, 72.80.Rj

It is well-known that half-filled conducting chains are unstable against a doubling of the unit cell, where the bond length between neighboring lattice sites alternates along the chain (dimerization). The resulting alternation of the electron hopping amplitudes opens a gap in the electron spectrum, turning the system into a semiconductor (Peierls instability) [1]. The phonons relevant for this instability have wave vector $q \sim \pi/a$ (a is the distance between neigboring lattice sites). These phonons backscatter electrons from the left part of the one-dimensional Fermi surface (wave vector $k \sim -\frac{\pi}{2a}$) to the right one ($k \sim \frac{\pi}{2a}$) and vice versa. It is usually assumed that above the phase transition temperature T_c these phonons have a finite frequency and we will, therefore, refer to them as optical phonons. Due to the mixing with the low-energy electron-hole excitations, these phonons soften and at T_c their frequency vanishes (giant Kohn anomaly) [2].

In this Letter we show that acoustic phonons (i.e. phonons of small wave vector q and small frequency $\omega_a(q) = v_0|q|$) may lead to a similar instability and that in the presence of both optical and acoustic phonons, the acoustic ones are the first to soften, independent of the coupling strengths involved. The acoustic component immobilizes the topological excitations (kinks) over the ordered state, while the softening leads to a sharp increase of the electrical resistivity just above T_c.

At first sight, acoustic phonons cannot open an electronic gap, as they only have small wave vectors, which does not allow for backscattering. This argument no longer holds, however, in lattices where the unit cell already contains two sites above T_c (where the electron hopping amplitude is still uniform along the chain), as in that situation the phonon wave vector is only conserved up to a multiple of $\frac{\pi}{a}$. For instance, due to its zigzag structure the undistorted *trans*-polyacetylene chain has lattice period $2a$ (Fig. 1(a)). In Fig. 1(b) it is shown how a small-q distortion perpendicular to the chain leads to bond-length alternation, which results in backscattering of electrons. We note that in the strictly one-dimensional Su-Schrieffer-Heeger model [3] of *trans*-polyacetylene, this acoustic backscattering cannot occur.

Another example is provided by an armchair single-wall carbon nanotube (CNT) (Fig. 1(c)). The undistorted armchair CNT has two half-filled one-dimensional electronic bands and is metallic [4]. Its unit cell contains two inequivalent carbon atoms, which gives rise to backscattering of electrons off acoustic phonons. The relevant acoustic phonons are the so-called twistons. It is easy to see that a uniform twist of the armchair CNT results in an alternation of the carbon-carbon bond lengths along the nanontube (Fig. 1(d)), which opens a gap in the spectrum of electron excitations. The scattering of electrons on twistons has recently been used to explain the linear temperature dependence of the resisitivity of a single-wall CNT [5].

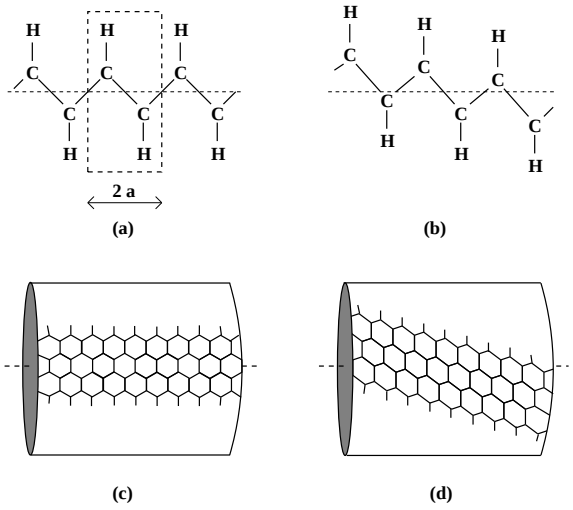

FIG. 1. The zigzag structure of *trans*-polyacetylene with two carbon atoms per unit cell, without lattice distortion (a) and with a small-wave-vector (acoustic) deformation perpendicular to the chain (b). Similarly, the undistorted armchair CNT (c) consists of connected zigzag chains in the tube direction. A twist deformation of the CNT leads to an out of phase alternation of the bond lengths in neighbouring chains.

The Hamiltonian of our model has the form,

$$H = \sum_{n\sigma} \int dx \Psi^\dagger_{n\sigma} \left\{ \frac{v_F}{i} \hat{\sigma}_3 \frac{\partial}{\partial x} + (\Delta_o + \Delta_a)\hat{\sigma}_1 \right\} \Psi_{n\sigma} + H_{lat}[\Delta_o] + H_{lat}[\Delta_a], \quad (1)$$

where the first term describes the kinetic energy of electrons close to the Fermi points and the backscattering

of the electrons due to the lattice modulation induced by both optical and acoustic phonons. Here, $\hat{\sigma}_1$ and $\hat{\sigma}_3$ are the Pauli matrices and we set $\hbar = 1$. The spinor $\Psi_{n\sigma} = \binom{\psi_{Rn\sigma}}{\psi_{Ln\sigma}}$ describes electrons moving to the right/left with the Fermi velocity v_F. We have omitted scattering contributions that leave the electron on the same side of the Fermi surface ($R \to R$ and $L \to L$), as these processes do not lead to an instability. The index $n = 1, \ldots, N_b$ denotes the electron band. The second and the third terms in Eq.(1) describe the energy of the optical ($i = o$) and acoustic ($i = a$) phonons,

$$H_{lat}[\Delta_i] = \frac{N_b}{\pi\lambda_i v_F}\int dx\, \Delta_i^2 + \frac{1}{2\rho_i}\int dx\, \pi_i^2, \qquad (2)$$

where the dimensionless coupling constant λ_i absorbs a factor N_b for the number of electron bands, and ρ_i is the mass density. The momentum density π_i is related to the phonon amplitude u_i by: $\pi_i(x,t) = \rho_i \partial u_i(x,t)/\partial t$.

In the continuum description of the optical and acoustic phonons coupled to electrons, Δ_i is related to the phonon amplitude u_i by

$$\begin{cases} \Delta_o \propto u_o(x,t) & \text{for optical phonons,} \\ \\ \Delta_a \propto \frac{\partial}{\partial x} u_a(x,t) & \text{for acoustic phonons.} \end{cases} \qquad (3)$$

The difference between the optical and acoustic phonons is due to the fact that the "order parameter" Δ incorporates also the electron-phonon coupling constant, as is clear from Eq. (1). While the coupling $g_a(q)$ to the acoustic phonon with wave vector q is proportional to q, the coupling to the optical phonon, $g_o(q)$, is approximately constant. At the same time, Eq. (3) gives the linear dispersion for acoustic phonons, $\omega_a = v_0|q|$, and a finite frequency ω_o for optical phonons. We note that, though the coupling to acoustic phonons $g_a(q)$ is small for small q, the actual strength of the interaction is given by the dimensionless coupling $\lambda_i \propto g_i^2/(v_F\omega_i^2)$, which is finite both for optical and acoustic phonons.

For $\Delta_a = 0$ and $N_b = 1$ the Hamiltonian Eq. (1) coincides with the Hamiltonian of the TLM model [6], which is the continuum version of the Su-Schrieffer-Heeger model [3] of *trans*-polyacetylene with one electron band. On the other hand, for $\Delta_o = 0$ and $N_b = 2$, the Hamiltonian Eq. (1) is equivalent to the Hamiltonian describing the electron-twiston interactions in the armchair CNTs [7,5].

Phase transition.—First we consider the temperature dependence of the optical and acoustic phonon frequencies for $T > T_c$. The bare phonon propagation $\hat{D}_0$ and the the coupling $\hat{V}$ to electrons is formally written in terms of 2×2-matrices,

$$\hat{D}_0 = \begin{pmatrix} D_a^0 & 0 \\ 0 & D_o^0 \end{pmatrix} \quad \text{and} \quad \hat{V} = \begin{pmatrix} g_a\, g_a^* & g_a\, g_o^* \\ g_o\, g_a^* & g_o\, g_o^* \end{pmatrix} P\,,$$

where $\hat{D}_0$ contains the bare acoustic and optical phonon propagators D_a^0 and D_o^0. The coupling $\hat{V}$ of the phonons to electrons has two effects: It mixes the bare optical and acoustic phonon modes and renormalizes their frequencies due to an electron-hole excitation that is described by the bare vacuum polarization $P = P(q,\omega,T)$ [8]. Within the random phase approximation, the propagation of dressed phonons is described by a matrix $\hat{D}$ that solves the Dyson equation $\hat{D} = \hat{D}_0 + \hat{D}_0\hat{V}\hat{D}$. The renormalized phonon frequencies $\tilde{\omega}_o(q)$ and $\tilde{\omega}_a(q)$ are found from the poles of $\det(\hat{D})$, or equivalently by solving $\det(\hat{D}_0^{-1} - \hat{V}) = 0$. Using that $\tilde{\omega}_a(q) \ll T$ and $\tilde{\omega}_a(q) \ll \tilde{\omega}_o(q)$, we eventually find:

$$\tilde{\omega}_a^2(q) = \omega_a^2(q)\,\frac{1 - (\lambda_o + \lambda_a)\ln(\gamma W/\pi T)}{1 - \lambda_o \ln(\gamma W/\pi T)} \qquad (4)$$

for the acoustic phonon and, assuming that $\tilde{\omega}_o(q) \ll T$,

$$\tilde{\omega}_o^2(q) = \omega_o^2(q)\,(1 - \lambda_o \ln(\gamma W/\pi T)) \qquad (5)$$

for the optical phonon. Here, W is the energy cut-off of the order of the electron band width and $\gamma = 1.781072...$ is Euler's constant.

We thus see, that the expression for the renormalized optical frequency is independent of λ_a and is the same as in the absence of the coupling to acoustic phonons. On the other hand, the renormalized acoustic phonon frequency depends on the sum of λ_a and λ_o. As a result, the acoustic phonons "soften" first, at the critical temperature given by

$$T_c \;=\; \frac{\gamma}{\pi} W \exp\left(-\frac{1}{\lambda_a + \lambda_o}\right). \qquad (6)$$

As $\tilde{\omega}_a(q = 0) = 0$ at all temperatures, the "softening" in this case means vanishing of the acoustic phonon velocity at $T = T_c$. Thus, no matter how much the optical coupling constant is larger than the acoustic coupling constant, it is always the velocity of the acoustic phonon that becomes zero at the transition temperature, whereas the optical phonon frequency stays finite at $T = T_c$. This is a consequence of the mixing of the optical and acoustic phonons due to their interactions with electrons, which results in a repulsion between the frequencies of the two modes. As a result, the optical and acoustic branches can never cross and the singularity at T_c always occurs in the lower, i.e. acoustic, branch. A similar effect takes place in some ferroelectrics, in which the sound velocity vanishes at the transition temperature because of the mixing of the soft mode, describing the ferroelectric displacement of ions, to acoustic phonons [9]. We also note that, at first sight, Eq. (6) resembles the result for the Peierls temperature obtained in Ref. [10]. It should be kept in mind, however, that in that paper the various coupling constants λ_i correspond to contributions from scattering within different electron bands and are not associated with the presence of several phonon modes. The additive effect of the number of electron bands is implicit

in our result through the fact that both λ_o and λ_a are proportional to N_b.

Next we discuss the ordered state below T_c. Because the lattice distortions, corresponding to the optical and acoustic phonons, are coupled due to electron-phonon interactions, both order parameters, $\Delta_a(x)$ and $\Delta_o(x)$, should appear below the transition temperature. In the mean field treatment of the lattice one has to minimize the total free energy of the model Eq.(1) with respect to the two order parameters. The solutions of the resulting self-consistency equations have the following properties: (i) The sum of the optical and acoustic order parameters, $\Delta(x) = \Delta_o(x) + \Delta_a(x)$, satisfies the same Bogoliubov-de Gennes equations as the order parameter of the TLM model [6] with a single phonon mode, but with the coupling constant $\lambda = \lambda_o + \lambda_a$; (ii) The optical ($i = o$) and acoustic ($i = a$) order parameters are proportional to $\Delta(x)$:

$$\Delta_i(x) = \frac{\lambda_i}{\lambda}\Delta(x).$$

Thus, the solutions of the TLM model can be used to study the ordered state in our model. In particular, the order parameter for the homogeneous solution $\Delta(x) = \Delta_0$ at zero temperature has the value $\Delta_0 = \frac{\pi}{\gamma}T_c$, with T_c as in Eq. (6).

The homogeneous optical order parameter, Δ_o, is a "frozen" phonon mode, corresponding to a uniform dimerization of the chain. On the other hand, for acoustic phonons, the constant Δ_a corresponds to the linearly growing amplitude of ionic displacements: $u_a(x) \propto \Delta_a x$. Such a lattice distortion is not a "frozen" phonon mode, as it corresponds to large deviations of ions from their equilibrium positions in the high-temperature phase. In the case of CNTs, $\Delta_a = $ const. corresponds to a uniform twist of the CNT (see Fig. 1). Such a twist was, in fact, recently observed using STM [11].

Topological Excitations.—In the SSH model, where electrons interact with one optical phonon mode, domain walls (kinks) in the order parameter, corresponding to a change of sign of the lattice dimerization along the chain, constitute an interesting class of excitations [3]. In the continuum model, the analytical expression for the kink is given by [6]:

$$\Delta(x) = \Delta_0 \tanh\frac{x}{\xi_0}, \tag{7}$$

where $\xi_0 = \frac{v_F}{\Delta_0}$ is the correlation length.

The kink Eq. (7) also is a consistent solution of the Bogoliubov-de Gennes equations for the total order parameter in our model with both optical and acoustic phonons. For this kink, the optical and acoustic lattice distortions take the form:

$$\begin{cases} u_o(x) &= \quad \bar{u}_o \tanh\frac{x}{\xi_0}, \\ \\ u_a(x) &= \bar{u}_a \ln\cosh\frac{x}{\xi_0}. \end{cases} \tag{8}$$

Near the kink both the lattice dimerzation, described by $u_o(x)$, and the derivative of $u_a(x)$ change sign (see Fig. 2). In the case of a CNT, the latter corresponds to the change of the sign of the twist-angle from $-(\bar{u}_a/\xi_0)$ to $+(\bar{u}_a/\xi_0)$.

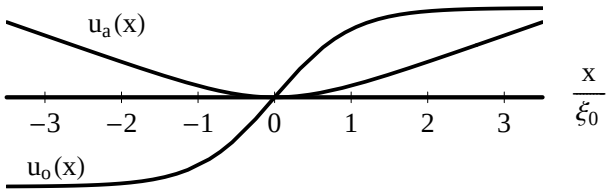

FIG. 2. Schematic plot of the optical ($u_o(x)$) and acoustic ($u_a(x)$) lattice distortions Eq. (8) corresponding to the topological excitation Eq. (7).

The creation energy of the kink in the model Eq.(1) is the same as for the kink in the TLM model [6]: $E_k = N_b(2\Delta_0/\pi)$. The dynamical properties of the kinks in these two models are, however, quite different. In the TLM model the kink can propagate with velocity v along the chain, without changing its profile. This results from the independence of the kink energy of its position and the fact that the kinetic energy density of the moving kink, $u_o(x,t) = \bar{u}_o \tanh\left(\frac{x-vt}{\xi_0}\right)$ decays exponentially at distances larger than ξ_0 from the kink. Thus, the mass of the kink (defined by equating the kinetic energy of the moving kink to $\frac{1}{2}Mv^2$) is finite and for *trans*-polyacetylene it was estimated to be $\sim 6m_e$ [3]. On the other hand, the motion of the kink in the model with acoustic phonons would result in a constant kinetic energy at distances larger than ξ_0 from the kink, as follows from the substitution of $u_a(x)$ in Eq.(8) by $u_a(x-vt)$. Thus, the mass of such a kink is proportional to the chain length L. This relates to the fact that a translation of the kink configuration Eq.(8) changes the coordinates of the chain ends, so that a shift of the kink induces a motion of the entire chain. Thus, in our model, isolated kinks cannot propagate along the chain. Kinks can propagate without affecting the chain ends only together with antikinks, the corresponding time-dependent lattice configuration being $u_R(x,t) = u_a(x-vt) - u_a(x+R-vt)$ [cf. Eq. (8)]. The mass of such a pair is proportional to the distance R between the kink and antikink.

Electrical conductivity.—Next we consider the temperature dependence of the electrical conductivity, $\sigma(T)$, above T_c. For $T \ll \tilde{\omega}_o$, the contribution of the optical phonons to the conductivity can be neglected. For $\lambda_a \ll \lambda_o$ this inequality may not be fulfilled close to T_c, as the renormalized optical phonon frequency at T_c, $\tilde{\omega}_o = \omega_o\sqrt{\lambda_a/(\lambda_a+\lambda_o)}$, may then be small. However, as we argue below, for CNTs, $\lambda_a \sim \lambda_o$, in which case there is no dramatic softening of the optical phonon and the conductivity close to T_c is also dominated by the electron backscattering off acoustic phonons.

The electrical conductivity is given by $\sigma(T) = (-4e^2 v_F/\pi) \int dk\, \tau_k (\partial n_F(v_F k)/\partial k)$, where n_F is the Fermi distribution and τ_k is the transport lifetime, which depends on the electron wave vector k. Using Fermi's Golden Rule and accounting for the renormalization Eq.(4) of the acoustic phonon frequency, we obtain

$$\tau_k = \frac{2}{\pi \lambda_a T} \left(\frac{\tilde{\omega}_a(2k)}{\omega_a(2k)} \right)^2 , \qquad (9)$$

where we have put $k_B = 1$.

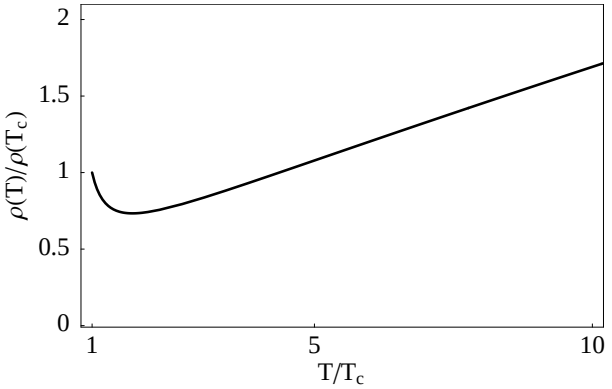

FIG. 3. The electrical resistivity $\rho = 1/\sigma$ as a function of temperature. The electron-phonon coupling strengths are chosen to be $\lambda_a = \lambda_o = 0.05$.

Fig. 3 shows the temperature dependence of the electrical resistivity, $\rho(T) = 1/\sigma(T)$, calculated for $T \geq T_c$ using Eq.(9). At temperatures $T \gg T_c$, the resistivity decreases linearly with temperature, $\rho(T) \propto \lambda_a T$, as was also found in Refs. [5,12]. However, close to T_c, due to the vanishing of the acoustic phonon velocity at the critical temperature, the resistivity strongly increases up to some finite value, $\rho(T_c)$. This behavior is very similar to the one observed for bundles of single-wall CNTs [5], where the cross-over between the linear decrease and the sharp upturn of the resistivity occurs at $T^* \sim 10 - 100$ K.

Usually, the Peierls instability is thought to be irrelevant for CNTs, because the electron-phonon coupling constant is inversely proportional to the number of zigzag chains, $2N$, in the armchair CNT, making T_c negligibly small for $N \geq 4$ [4]. We note, however, that previously only the interaction with optical phonons, *e.g.*, the deformations resulting in a Kekulé or quinoid type structure of the CNT lattice, was considered [4]. When we take into account the scattering of electrons on acoustic phonons (twistons), we obtain a higher value of the coupling constant λ $(= \lambda_o + \lambda_a)$, which gives a much higher value of T_c. In particular, using typical parameters for graphite [5], we obtain $\lambda_a \simeq 0.23/N$. Furthermore, if one assumes that the electron hopping amplitudes and the spring constants only depend on the carbon-carbon bond length, one finds $\lambda_o \sim \lambda_a$. For CNTs with $N = 4$, which were recently discussed in the context of possible technological applications [13], the critical temperature given by Eq. (6) is then ~ 10 K, instead of only a few mK for the Peierls transition temperature without acoustic phonons. We note, however, that the interaction of the CNTs with their environement (other CNTs and the substrate) may, in principle, suppress the Peierls instability.

The values of the electron-phonon coupling constants for a CNT could, in principle, be obtained from the form of the resistivity curve (λ_a determines the slope of $\rho(T)$ at high temperatures, whereas T_c depends on $\lambda_a + \lambda_o$). However, so far, such measurements have only been performed on bundles of nanotubes, in which one cannot control the radius and chirality of the CNTs. Therefore, measuring the resistivity of a single CNT would be very desirable.

Conclusions.—In this Letter we studied the Peierls transition resulting from electrons interacting with both optical and acoustic phonons. We found that, independent of the electron-phonon coupling constants, the acoustic phonon velocity vanishes at the critical temperature, whereas the optical phonon frequency remains finite. This is different from the conventional Peierls scenario, in which the optical phonon softens at T_c. We suggested that such a transition may take place in CNTs of small radius, leading to a static twist below T_c. The temperature dependence of the resistivity calculated within our model qualitatively agrees with experimental data on CNTs. Unlike the topological excitations in *trans*-polyacetylene, the kinks in our model are immobile even in isolated chains and can propagate only in pairs. Finally we note that, though we used CNTs as a specific example, we believe that our results have a more general significance.

We gratefully acknowledge financial support by the Stichting Fundamenteel Onderzoek der Materie (FOM).

[1] R.E. Peierls, *"Quantum Theory of Solids"* (Clarendon, Oxford, 1955).
[2] M.J. Rice and S. Strässler, Solid State Commun. **13**, 125 (1973).
[3] A.J. Heeger, S. Kivelson, J.R. Schrieffer, and W.P. Su, Rev. Mod. Phys. **60**, 781 (1988).
[4] *for a review see:* R. Saito, G. Dresselhaus, and M.S. Dresselhaus, *Physical Properties of Carbon Nanotubes*, Imperial College Press (1998).
[5] C.L. Kane, *et al.*, Europhysics Letters **41**, 683 (1998).
[6] H. Takayama, Y.R. Lin-Liu, and K. Maki, Phys. Rev. B **21**, 2388 (1980).
[7] C.L. Kane and E.J. Mele, Phys. Rev. Lett. **78**, 1932 (1997).
[8] G.D. Mahan, *Many-Particle Physics*, pp. 156, Plenum Press, New York (1981).
[9] E. M. Brody and H. Z. Cummings, Phys. Rev. Lett. **21**,

1263 (1968).
[10] Y. Huang, *et al.*, Solid State Commun. **97**, 303 (1996).
[11] W. Clauss, *et al.*, Phys. Rev. B **58**, R4266 (1998).
[12] R.A. Jishi, M.S. Dresselhaus, G. Dresselhaus, Phys. Rev. B **48**, 11385 (1993).
[13] A.A. Farajian, K. Esfarjani, and Y. Kawazoe, Phys. Rev. Lett. **82**, 5084 (1999).